

Long-lived Bino and Wino in supersymmetry with heavy scalars and higgsinos

Krzysztof Rolbiecki^a and Kazuki Sakurai^b

^a*Instituto de Física Teórica, IFT-UAM/CSIC,
C/ Nicolás Cabrera, 13-15, Cantoblanco, 28049 Madrid, Spain*

^b*Department of Physics, King's College London, London WC2R 2LS, UK*

E-mail: krzysztof.rolbiecki@desy.de, kazuki.sakurai@kcl.ac.uk

ABSTRACT: We point out that there is a parameter region in supersymmetry with heavy scalars and higgsinos, in which the heavier of the Bino and the Wino becomes long-lived as a consequence of the heavy higgsinos. In this region these electroweak gaugino sectors are secluded each other with very small mixings that are inversely proportional to the higgsino mass. We revisit the Bino and Wino decays and provide simple formulae for the partial decay rate and the lifetime in the limit of heavy higgsinos. We briefly discuss the collider signature of the long-lived Bino and Winos in this scenario.

KEYWORDS: Supersymmetry Phenomenology, Hadronic Colliders

Contents

1	Introduction	1
2	Interaction between Wino and Bino	2
3	Two body decays	4
3.1	Wino NLSP case ($ M_2 > M_1 $)	4
3.2	Bino NLSP case ($ M_1 > M_2 $)	6
4	Three body decays	7
4.1	Wino NLSP case ($ M_2 > M_1 $)	7
4.2	Bino NLSP case ($ M_1 > M_2 $)	11
5	Large mass splitting between gauginos and higgsinos	12
6	Collider signatures	13
7	Conclusion	14
A	The three body decay rate of the neutral Wino	15
B	The functions	16

1 Introduction

Supersymmetry (SUSY) remains as a promising new physics candidate after LHC run-I. The discovery of the Higgs boson with $m_h \simeq 125$ GeV and the negative results of the new physics searches at the LHC make the SUSY scenario with heavy scalars more attractive. In this scenario, scalars (except for the Standard Model (SM) like Higgs boson, h) are heavier than the TeV scale and the observed Higgs mass can be easily realised by the large correction from the heavy scalars [1–3]. The gauge coupling unification can be achieved with the light gauginos [4] and such light gauginos can be within the reach of the collider experiments. If the Wino is the lightest SUSY particle (LSP), the thermal relic abundance bounds the Wino mass from above by 2.7 TeV [5, 6]. The splitting between the scalar and gaugino masses is also motivated by model building. If the SUSY breaking field with non-vanishing F -term is charged under some symmetry, only scalars acquire the soft masses at tree-level. The gaugino masses can be generated from other contributions such as the anomaly mediated contribution, but they are parametrically smaller than the scalar mass.

It has been pointed out that gluinos can be long-lived in this scenario if quarks are heavier than $\mathcal{O}(10^3)$ TeV [4]. Such long-lived gluinos, if produced, may leave a distinctive

R-hadron signature or a signature of displaced gluino decays [7, 8]. With decoupled squarks, the $SU(3)$ gaugino sector is secluded from the other gaugino sectors and the gluino becomes stable even if there exist lighter gauginos. The situation is somewhat different for the $SU(2)_L$ and $U(1)_Y$ gauginos because of the electroweak symmetry breaking (EWSB). These sectors are mixed after the EWSB and a particle in the heavier gaugino sector can decay into lighter ones without mediation of scalars. However, this mixing is proportional to the ratio of the vacuum expectation value of the Higgs field, v ,¹ and the mass of the fermionic component of the Higgs field, μ , and can become arbitrarily small if the magnitude of μ increases.

In this paper we point out there is a parameter region in SUSY models with heavy scalars and higgsinos where the heavier of Wino and Bino becomes long-lived as a consequence of the large μ parameter. We revisit the decays of electroweak gauginos and derive simple formulae for the partial decay rate and the lifetime, which are valid in the limit of the heavy higgsinos. We identify the region where the Bino and Winos become long-lived for both cases of two- and three-body decays.

This paper is organised as follows: in the following section we review the chargino and neutralino sectors in the minimal SUSY Standard Model (MSSM) and study the mixings and interactions between the Bino and Winos in the heavy higgsino limit. We then revisit the decays of the Bino and Winos for the two- and three-body decays in sections 3 and 4, respectively. In these sections, we identify the scale of μ , in which the Bino and Winos have a collider scale lifetime. In section 5 we briefly discuss how the large mass splitting between the gauginos and higgsinos can be theoretically achieved. The collider signature of the long-lived Bino and Winos in our scenario is briefly discussed in section 6. Section 7 is devoted to conclusion.

2 Interaction between Wino and Bino

The chargino mass matrix is given by²

$$\mathcal{M}_C = \begin{pmatrix} M_2 & \sqrt{2}m_W s_\beta \\ \sqrt{2}m_W c_\beta & \mu \end{pmatrix}, \quad (2.1)$$

where c_β (s_β) represents $\cos \beta$ ($\sin \beta$) and β is defined as the ratio of the vacuum expectation values of two Higgs fields, $\tan \beta = \langle H_u \rangle / \langle H_d \rangle$. This matrix can be diagonalised as $\mathcal{M}_C^{\text{diag}} = U^* \mathcal{M}_C V^{-1}$ where U and V take the following forms

$$U \simeq \begin{pmatrix} 1 & -\frac{\sqrt{2}s_\beta m_W}{\mu} \\ \frac{\sqrt{2}s_\beta m_W}{\mu} & 1 \end{pmatrix}, \quad V \simeq \begin{pmatrix} 1 & -\frac{\sqrt{2}c_\beta m_W}{\mu} \\ \frac{\sqrt{2}c_\beta m_W}{\mu} & 1 \end{pmatrix}, \quad (2.2)$$

in the large μ limit. The eigenvalues are given by

$$m_{\tilde{W}^\pm} \simeq M_2, \quad m_{\tilde{\chi}_2^\pm} \simeq |\mu|, \quad (2.3)$$

¹ More precisely v^2 is defined by the square sum of the two Higgs field vevs: $v^2 = \langle H_u \rangle^2 + \langle H_d \rangle^2$.

² We closely follow the calculation and convention used in [9, 10].

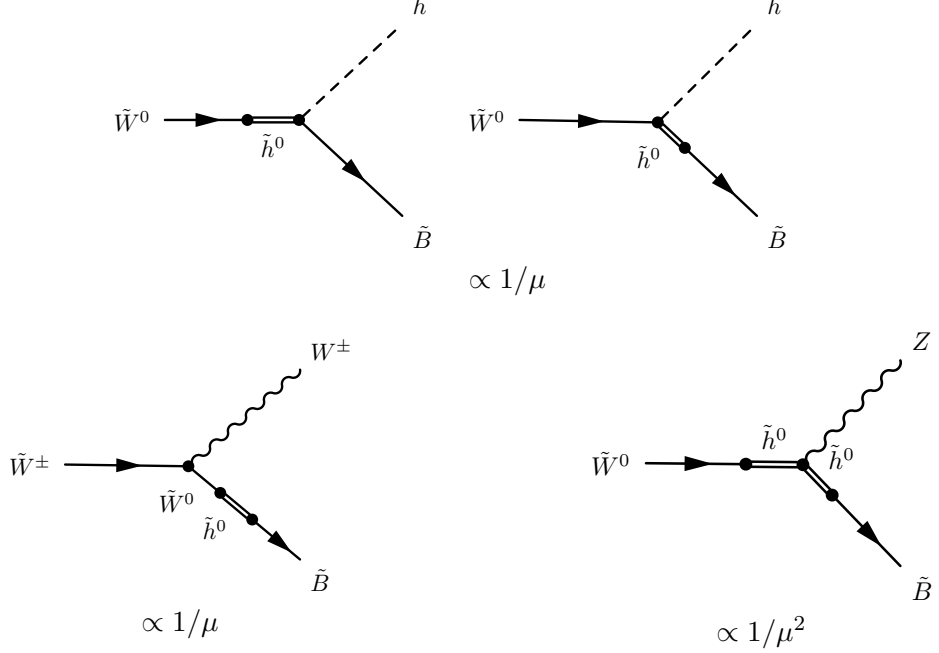


Figure 1. The Wino-Bino interaction with the Higgs and gauge bosons.

with $m_{\tilde{W}^\pm} \ll m_{\tilde{\chi}_2^0}$.

The neutralino mass matrix is given by

$$\mathcal{M}_N = \begin{pmatrix} M_1 & 0 & -m_Z s_W c_\beta & m_Z s_W s_\beta \\ 0 & M_2 & m_Z c_W c_\beta & -m_Z c_W s_\beta \\ -m_Z s_W c_\beta & m_Z c_W c_\beta & 0 & -\mu \\ m_Z s_W s_\beta & -m_Z c_W s_\beta & -\mu & 0 \end{pmatrix}. \quad (2.4)$$

In the large μ limit, the diagonalising matrix Z can be written as

$$Z \simeq \begin{pmatrix} 1 & -\frac{m_Z^2 s_W s_{2\beta}}{2\mu(M_2 - M_1)} & \frac{m_Z s_W s_\beta}{\mu} & -\frac{m_Z s_W c_\beta}{\mu} \\ \frac{m_Z^2 s_W s_{2\beta}}{2\mu(M_2 - M_1)} & 1 & -\frac{m_Z c_W s_\beta}{\mu} & \frac{m_Z c_W c_\beta}{\mu} \\ \frac{m_Z s_W (c_\beta - s_\beta)}{\sqrt{2}\mu} & -\frac{m_Z c_W (c_\beta - s_\beta)}{\sqrt{2}\mu} & \frac{1}{\sqrt{2}} & \frac{1}{\sqrt{2}} \\ \frac{m_Z s_W (c_\beta + s_\beta)}{\sqrt{2}\mu} & -\frac{m_Z c_W (c_\beta + s_\beta)}{\sqrt{2}\mu} & -\frac{1}{\sqrt{2}} & \frac{1}{\sqrt{2}} \end{pmatrix}, \quad (2.5)$$

where s_W is the Weinberg angle, $\sin \theta_W$, and $c_W \equiv \cos \theta_W$. The mass eigenvalues are found as

$$m_{\tilde{B}} \simeq M_1, \quad m_{\tilde{W}^0} \simeq M_2, \quad m_{\tilde{\chi}_3^0} \simeq m_{\tilde{\chi}_4^0} \simeq |\mu|, \quad (2.6)$$

where $m_{\tilde{B}}, m_{\tilde{W}^0} \ll m_{\tilde{\chi}_3^0}, m_{\tilde{\chi}_4^0}$.

The Wino and Bino interact each other with a Higgs or a gauge boson through the mixing matrices U , V and Z . The interaction with the Higgs boson, h , is dictated by the $\tilde{\chi}_j^0$ - $\tilde{\chi}_i^0$ - h coupling [10]

$$G_{ijh}^L = G_{ijh}^R = -\frac{1}{2s_W}(Z_{j2} - \tan \theta_W Z_{j1})(\sin \alpha Z_{i3} + \cos \alpha Z_{i4}) + i \leftrightarrow j, \quad (2.7)$$

where α is the mixing angle of the neutral Higgs sector and reduces to $\sin \alpha = c_\beta$, $\cos \alpha = -s_\beta$ in the decoupling limit of the SUSY Higgses. In the large μ limit these couplings can be reduced to

$$G_{\tilde{W}^0 \tilde{B} h} \simeq \frac{1}{2s_W} \left[(c_\beta Z_{13} - s_\beta Z_{14}) - \frac{s_W}{c_W} (c_\beta Z_{23} - s_\beta Z_{24}) \right] \simeq \frac{m_Z s_{2\beta}}{\mu}. \quad (2.8)$$

This interaction is illustrated diagrammatically in the bottom-left graph in Fig. 1. We note that the coupling is originated from the Bino-higgsino and Wino-higgsino mixing and suppressed by m_Z/μ for large μ .

The interaction with the W boson is found in the $\tilde{\chi}_j^\pm \tilde{\chi}_i^0 W^\mp$ coupling

$$G_{ijW}^L = \frac{1}{s_W} (Z_{i2} V_{j1} - \frac{1}{\sqrt{2}} Z_{i4} V_{j2}), \quad G_{ijW}^R = \frac{1}{s_W} (Z_{i2} U_{j1} + \frac{1}{\sqrt{2}} Z_{i3} U_{j2}), \quad (2.9)$$

and in the large μ limit these couplings can be written as

$$G_{\tilde{B} \tilde{W}^\pm W} \simeq -\frac{m_Z^2 c_W s_{2\beta}}{\mu(M_2 - M_1)}. \quad (2.10)$$

The interaction is depicted in the bottom-left graph in Fig. 1. The coupling is proportional to m_Z/μ and originated from the Bino-Wino mixing, Z_{12} .

We illustrate the Wino-Bino interaction with the Z boson in the bottom-right graph in Fig. 1. Unlike the other interactions, this coupling requires both the Wino-higgsino and the Bino-higgsino interaction. Formally the interaction is found in the $\tilde{\chi}_j^0 \tilde{\chi}_i^0 Z$ coupling

$$G_{ijZ}^R = -G_{ijZ}^L = \frac{1}{s_{2W}} (Z_{i3} Z_{j3} - Z_{i4} Z_{j4}), \quad (2.11)$$

and these couplings are reduced in the large μ limit to

$$G_{\tilde{W}^0 \tilde{B} Z}^R = -G_{\tilde{W}^0 \tilde{B} Z}^L \simeq \frac{m_Z^2 c_{2\beta}}{2\mu^2}. \quad (2.12)$$

These couplings are proportional to $(m_Z/\mu)^2$ and become small much more quickly than the other couplings as $|\mu|$ increases. There exists another contribution to the Bino-Wino- Z interaction from higher order terms. The higgsino-Higgs loop diagram generates the dimension 5 operator

$$\tilde{B} \tilde{W}^a \sigma^{\mu\nu} F_{\mu\nu}^a. \quad (2.13)$$

A naive dimensional analysis suggests that the coefficient of this operator is proportional to $\alpha/(4\pi\mu)$. Although this contribution is suppressed by the loop factor, it can easily dominate the tree-level interaction eq. (2.12) for very large μ . We will come back to this point later in this paper.

3 Two body decays

3.1 Wino NLSP case ($|M_2| > |M_1|$)

Throughout this paper, we assume gluinos are heavier than the Wino and the Bino. If Winos are heavier than the Bino and the mass difference is large, the charged and neutral Winos decay into a SM-boson and a Bino.

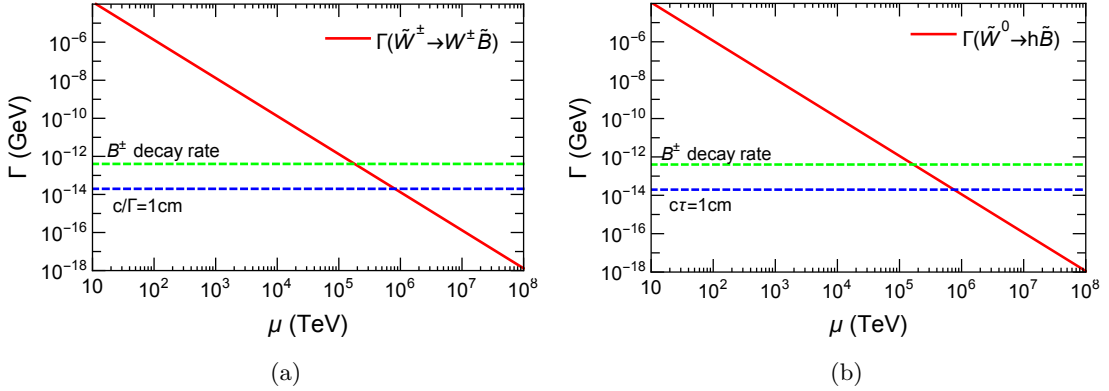


Figure 2. The decay rate of Winos. $M_2 = 800$ GeV, $M_1 = 300$ GeV, $\tan \beta = 2$.

The decay of the charged Wino is induced from the bottom-left diagram in Fig. 1, which leads to the final state of W^\pm and \tilde{B} . The decay rate of this process is given by [10]

$$\begin{aligned} \Gamma(\tilde{W}^\pm \rightarrow W^\pm \tilde{B}) &= \frac{\alpha}{4} M_2 G_{\tilde{B} \tilde{W}^\pm W}^2 f_-(\mu_{\tilde{B}}, \mu_w) \\ &\simeq \frac{\alpha s_{2\beta}^2 M_2}{4} \frac{m_Z^2}{\mu^2} \left[\frac{m_W^2 f_-(\mu_{\tilde{B}}, \mu_V)}{(M_2 - M_1)^2} \right] \\ &\sim \frac{\alpha}{4} (M_2 - M_1) s_{2\beta}^2 \frac{m_Z^2}{\mu^2} \left(1 + \frac{M_1}{M_2}\right)^3 \end{aligned} \quad (3.1)$$

where $\mu_{\tilde{B}} = M_1^2/M_2^2$ and $\mu_w = m_W^2/M_2^2$. The analytic expression of $f_-(x, y)$ is given in Appendix B. Throughout this section and the following section, the second formula starting with “ \simeq ” is an approximated expression valid for the large μ limit. In the third line we further approximate the expression assuming $\mu_w \ll 1$. Using the last expression, the lifetime of the charged Wino is found as

$$c\tau_{\tilde{W}^\pm} \sim 2.5 \text{ cm} \cdot \left(\frac{\mu}{10^6 \text{ TeV}} \right)^2 \left(\frac{500 \text{ GeV}}{M_2 - M_1} \right) \left(\frac{1}{s_{2\beta}} \right)^2 \left(\frac{M_2}{M_2 + M_1} \right)^3. \quad (3.2)$$

We show in Fig. 2(a) the decay rate of \tilde{W}^\pm as a function of $|\mu|$. The horizontal green line represents the decay rate of B^\pm meson as a reference, where the displacement of the \tilde{W}^\pm decay from the primary vertex starts to be visible. The horizontal blue line corresponds to the decay rate where the $c/\Gamma = 1$ cm, where the charged Winos start to reach the trackers leaving the distinctive kink-like signature. As can be seen, the charged Wino has a collider scale lifetime for $|\mu| \gtrsim 10^5$ TeV, if the two body $\tilde{W}^\pm \rightarrow W^\pm \tilde{B}$ is kinematically allowed.

There are two possible decay modes for the neutral Wino: $\tilde{W}^0 \rightarrow Z \tilde{B}$ and $\tilde{W}^0 \rightarrow h \tilde{B}$. The former is induced from the bottom-right diagram in Fig. 1 and the dimension 5 operator in eq. (2.13). However these contributions are suppressed by the extra (m_Z/μ) factor and the loop factor in the matrix element level, respectively, compared to the $\tilde{W}^0 \rightarrow h \tilde{B}$ decay.

Therefore if the mass difference is large enough to allow the two body $\tilde{W}^0 \rightarrow h\tilde{B}$ decay, the neutral Wino predominantly decays into h and \tilde{B} . The decay rate is given by

$$\begin{aligned}\Gamma(\tilde{W}^0 \rightarrow h\tilde{B}) &= \frac{\alpha}{4} M_2 G_{\tilde{W}^0\tilde{B}h}^2 f_h(\mu_{\tilde{B}}, \mu_h) \\ &\simeq \frac{\alpha M_2}{4} s_{2\beta}^2 \frac{m_Z^2}{\mu^2} f_h(\mu_{\tilde{B}}, \mu_h) \\ &\sim \frac{\alpha}{4} (M_2 - M_1) s_{2\beta}^2 \frac{m_Z^2}{\mu^2} \left(1 + \frac{M_1}{M_2}\right)^3\end{aligned}\quad (3.3)$$

where $\mu_h = m_h^2/M_2^2$, and the analytic expression of $f_h(x, y)$ is given in Appendix B. We approximate the formula with the $\mu_h \ll 1$ assumption in the third line. It is noted that the last expression is identical to the one in eq. (3.1). This can be also seen in Fig. 2(b), where we show the decay rate of \tilde{W}^0 as a function of $|\mu|$. The approximate lifetime formula for the \tilde{W}^0 is therefore also given in eq. (3.2) with $c\tau_{\tilde{W}^0} \sim c\tau_{\tilde{W}^\pm}$. At colliders the long-lived neutral Wino leaves the displaced dijet/jets signatures [11, 12].

We would like to comment on the special case where $m_Z < |M_2| - |M_1| < m_h$. In this case the $\tilde{W}^0 \rightarrow h\tilde{B}$ decay is kinematically forbidden and the \tilde{W}^0 decays predominantly into Z and \tilde{B} , through the bottom-right diagram in Fig. 1 and the dimension 5 operator in eq. (2.13). Since the tree-level contribution is suppressed by the extra $1/\mu$ factor, the contribution from the dimension 5 operator dominates in the large $|\mu|$ region. This parameter region is interesting because the neutral Wino can be long lived with much smaller $|\mu|$. We leave this study for future work.

3.2 Bino NLSP case ($|M_1| > |M_2|$)

If the Bino is heavier than the Winos, the Bino can decay either to W^\pm plus a charged Wino and h or Z plus a neutral Wino. As we discussed in the subsection, the interaction of \tilde{B} - \tilde{W} - Z is suppressed compared to those for \tilde{B} - \tilde{W} - W and \tilde{B} - \tilde{W} - h , and the Bino decay is dominated by the W and h decay modes. The partial decay rates for these modes are given by

$$\begin{aligned}\Gamma(\tilde{B} \rightarrow \tilde{W}^\pm W^\mp) &= \frac{\alpha}{2} M_1 G_{\tilde{B}\tilde{W}^\pm W}^2 f_-(\mu_{\tilde{W}}, \mu_w) \\ &\simeq \frac{\alpha s_{2\beta}^2 M_1}{2} \frac{m_Z^2}{\mu^2} \left[\frac{m_W^2 f_-(\mu_{\tilde{W}}, \mu_w)}{(M_1 - M_2)^2} \right], \\ &\sim \frac{\alpha}{2} (M_1 - M_2) s_{2\beta}^2 \frac{m_Z^2}{\mu^2} \left(1 + \frac{M_2}{M_1}\right)^3,\end{aligned}\quad (3.4)$$

and

$$\begin{aligned}\Gamma(\tilde{B} \rightarrow h\tilde{W}^0) &= \frac{\alpha}{4} M_1 G_{\tilde{W}^0\tilde{B}h}^2 f_h(\mu_{\tilde{W}}, \mu_h), \\ &\simeq \frac{\alpha M_1}{4} s_{2\beta}^2 \frac{m_Z^2}{\mu^2} f_h(\mu_{\tilde{W}}, \mu_h), \\ &\sim \frac{\alpha}{4} (M_1 - M_2) s_{2\beta}^2 \frac{m_Z^2}{\mu^2} \left(1 + \frac{M_2}{M_1}\right)^3,\end{aligned}\quad (3.5)$$

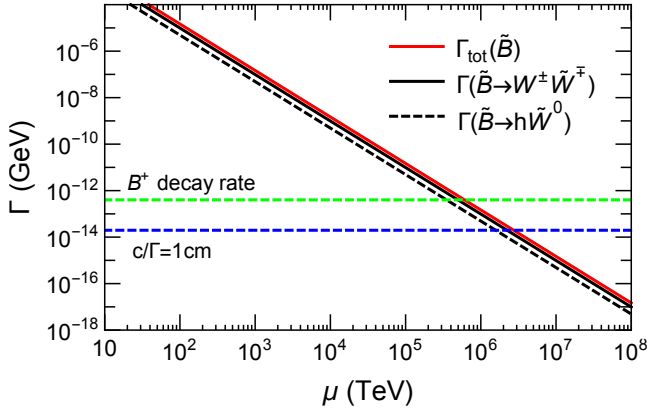


Figure 3. The decay rate of Bino. $M_1 = 800$ GeV, $M_2 = 300$ GeV, $\tan \beta = 2$.

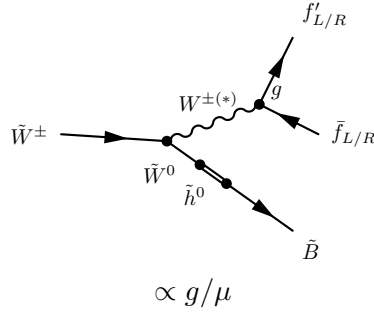


Figure 4. Diagram for $\tilde{W}^\pm \rightarrow W^\pm \tilde{B}$ decay.

where $\mu_{\tilde{W}} = M_2^2/M_1^2$, $\mu_w = m_W^2/M_1^2$ and $\mu_h = m_h^2/M_1^2$. The last expressions starting with “~” are approximated for the $\mu_w \ll 1$ and $\mu_h \ll 1$ cases, respectively. If $\mu_h \ll 1$, we find the universality

$$Br(\tilde{B} \rightarrow W^+ \tilde{W}^-) \sim Br(\tilde{B} \rightarrow W^- \tilde{W}^+) \sim Br(\tilde{B} \rightarrow h \tilde{W}^0) \sim 1/3. \quad (3.6)$$

Fig. 3 shows the total and partial decay rates for the Bino as a function of $|\mu|$. One can see that the Bino can be long lived if $|\mu| \gtrsim 10^6$ TeV. The Bino lifetime is approximately given as

$$c\tau_{\tilde{B}} \sim 1 \text{ cm} \cdot \left(\frac{\mu}{10^6 \text{ TeV}} \right)^2 \left(\frac{500 \text{ GeV}}{M_1 - M_2} \right) \left(\frac{1}{s_{2\beta}} \right)^2 \left(\frac{M_1}{M_1 + M_2} \right)^3. \quad (3.7)$$

4 Three body decays

4.1 Wino NLSP case ($|M_2| > |M_1|$)

In this section we consider the cases where the Bino and Wino mass difference is small and the two body decay modes considered in the previous section are kinematically not allowed.

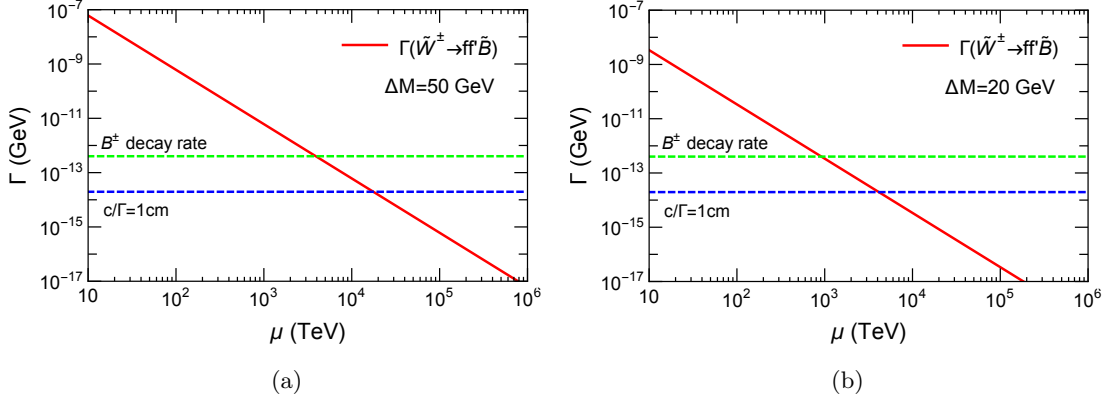


Figure 5. The decay rate of the charged Wino as a function of $|\mu|$. The other parameters are fixed at $M_2 = M_1 + \Delta M$, $M_1 = 500$ GeV, $\tan \beta = 2$.

We start with the $|M_2| > |M_1|$ case and define the mass difference $\Delta M \equiv |M_2| - |M_1| > 0$. If $\Delta M < m_W$ the charged Wino two body decay, $\tilde{W}^\pm \rightarrow W^\pm \tilde{B}$, is forbidden. In this case, the charged Wino decays into a pair of fermions and a Bino, though an off-shell W as shown in Fig. 4. The decay rate of this process is given by

$$\begin{aligned} \Gamma_f(\tilde{W}^+ \rightarrow f \bar{f}' \tilde{B}) &= \frac{\alpha^2 M_2}{16\pi} \frac{1}{s_W^2} \cdot G_{\tilde{B} \tilde{W}^\pm W}^2 \cdot \Omega_-(\mu_{\tilde{B}}, \mu_w), \\ &\simeq \frac{\alpha^2 M_2}{16\pi} \frac{s_{2\beta}^2}{s_W^2} \frac{m_Z^2}{\mu^2} \left[\frac{m_W^2 \Omega_-(\mu_{\tilde{B}}, \mu_w)}{(M_2 - M_1)^2} \right], \\ &\sim \frac{4\alpha^2}{15\pi} \frac{(\Delta M)^3}{\mu^2} \frac{s_{2\beta}^2}{s_{2W}^2}, \end{aligned} \quad (4.1)$$

where $\mu_w = m_W^2/M_2^2$ and the analytic expression of $\Omega_\pm(x, y)$ is given in Appendix B. In the last formula we approximate the expression assuming $\Delta M/M_2 \ll 1$. We may naively expect the decay rate should be proportional to $(\Delta M)^5/m_W^4$ due to the s -channel structure. However the Wino-Bino mixing, Z_{12} , is inversely proportional to the ΔM and the decay rate is finally proportional to the $(\Delta M)^3$.

We show the \tilde{W}^\pm decay rate, $\Gamma(\tilde{W}^\pm \rightarrow f \bar{f}' \tilde{B}) = \sum_f \Gamma_f(\tilde{W}^\pm \rightarrow f \bar{f}' \tilde{B})$, in Fig. 5(a) and 5(b) for $\Delta M = 50$ and 20 GeV, respectively. One can see that the charged Wino can be long lived for $|\mu| \gtrsim 10^{3-4}$ TeV depending on the mass splitting ΔM . The approximate formula for the charged Wino lifetime is given as

$$c\tau_{\tilde{W}^\pm} \sim 1 \text{ cm} \cdot \left(\frac{\mu}{10^4 \text{ TeV}} \right)^2 \left(\frac{30 \text{ GeV}}{\Delta M} \right)^3 \left(\frac{1}{s_{2\beta}} \right)^2. \quad (4.2)$$

We now turn to the three body decay of the neutral Wino for $\Delta M < m_Z$. In the previous section we have discussed that $\tilde{W} \cdot \tilde{B} \cdot Z$ coupling is suppressed by the extra m_Z/μ factor compared to the $\tilde{W} \cdot \tilde{B} \cdot h$, and the decay mode to the Higgs dominates the neutral

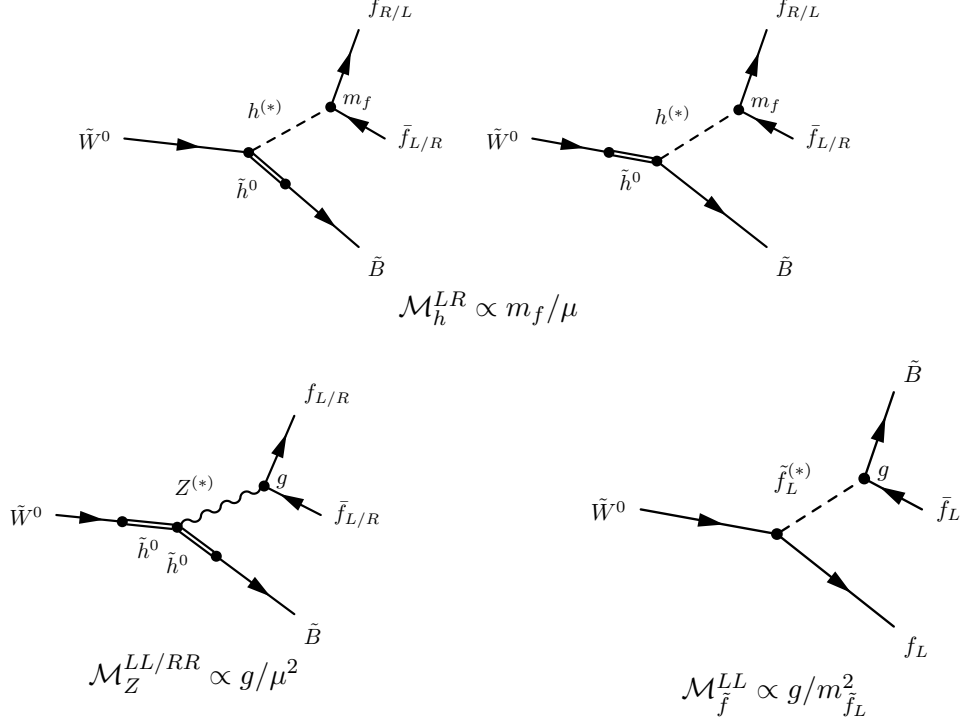


Figure 6. Diagrams contributing to the $\tilde{W}^0 \rightarrow f\bar{f}\tilde{B}$ decay.

Wino decay. In three body decay, however, the Higgs exchange diagram also receives a suppression, which is proportional to the mass of the final state fermions as shown in the upper diagrams in Fig. 6.

There are several competing contributions depending on the size of $|\mu|$. First, there is the Z -exchange diagram as shown in the lower left of Fig. 6. The matrix element of this diagram has the LL and RR chirality structure for the final state fermions and is proportional to $1/\mu^2$. If the mass of sfermions is the same size of $|\mu|$, the sfermion exchange diagram shown in the lower right of Fig. 6 can provide a sizeable contribution. The matrix element is inversely proportional to the squared mass of the left-handed sfermions, $m_{\tilde{f}_L}^2$. The contribution can interfere with the Z -exchange diagram since the matrix element has the LL structure. These contributions become significant if $|\mu|$ or $m_{\tilde{f}_L}^2$ is relatively small.

In order to conveniently address the importance of these contributions, we assume all the sfermion masses and $|\mu|$ have the same value M_X , and write the neutral Wino decay rate as

$$\Gamma(\tilde{W}^0 \rightarrow f\bar{f}\tilde{B}) \simeq \Gamma^{(2)}(\tilde{W}^0 \rightarrow f\bar{f}'\tilde{B}) + \Gamma^{(4)}(\tilde{W}^0 \rightarrow f\bar{f}'\tilde{B}), \quad (4.3)$$

where $\Gamma^{(2)}$ and $\Gamma^{(4)}$ represents the contributions that scale as $1/M_X^2$ and $1/M_X^4$, respectively.

We note that the Z -exchange contribution induced from the dimension 5 operator also has the scaling $1/M_X$ in the matrix element level and interfere with the tree-level Z and sfermion exchange contributions. We however neglect this contribution in this paper because the operator should be suppressed by the loop factor $\mathcal{O}(\alpha/4\pi)$, which is seemingly smaller than the m_f/m_W factor in the tree-level Higgs exchange contribution. The full

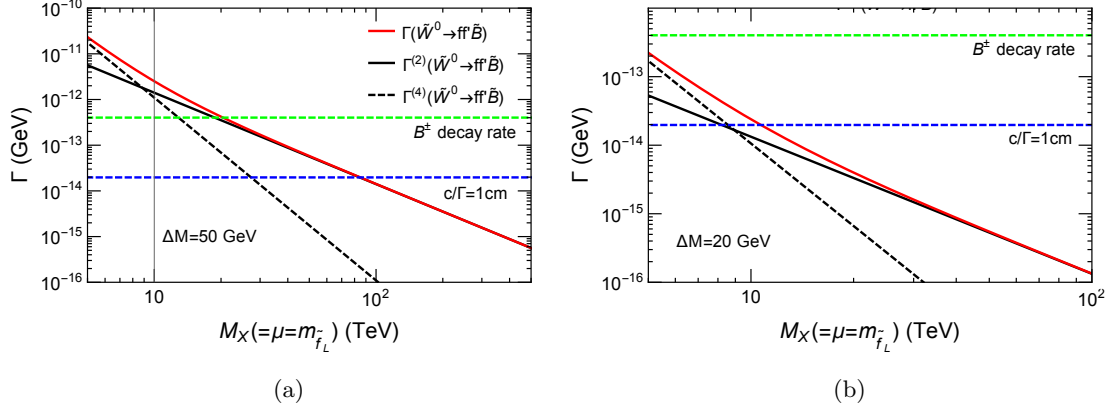


Figure 7. The decay rate of the neutral Wino as a function of $M_X (= |\mu| = m_{\tilde{f}_L})$. The other parameters are taken at $M_2 = M_1 + \Delta M$, $M_1 = 500$ GeV, $\tan \beta = 2$.

calculation including this higher order Z -exchange contribution is however important to precisely determine the lifetime of the neutral Wino, which is beyond the scope of this paper.

The partial decay rates $\Gamma^{(2)}(\tilde{W}^0 \rightarrow f \bar{f}' \tilde{B})$ and $\Gamma^{(4)}(\tilde{W}^0 \rightarrow f \bar{f}' \tilde{B})$ as well as the total decay rate $\Gamma(\tilde{W}^0 \rightarrow f \bar{f}' \tilde{B})$ are shown in Fig. 7(a) and 7(b) for $\Delta M = 50$ and 20 GeV, respectively, as functions of M_X . One can see that the neutral Wino can become long lived with $M_X \gtrsim 20$ TeV for the $\Delta M = 50$ GeV case and even with $M_X \gtrsim 5$ TeV for the $\Delta M = 20$ GeV case. The contribution from the Z and sfermion exchange diagrams, $\Gamma^{(4)}$, is negligible for very large μ . As decreasing M_X , this contribution starts to be significant around $M_X \sim 20$ TeV and becomes leading contribution from $M_X \lesssim 8$ TeV.

The analytic expression for the Higgs exchange contribution, $\hat{\Gamma}_f^h$, is given by

$$\begin{aligned}
 \hat{\Gamma}_f^h(\tilde{W}^0 \rightarrow f \bar{f}' \tilde{B}) &= \frac{\alpha^2 M_2}{32\pi} \frac{1}{s_W^2} \cdot \left(\frac{m_f}{m_W} r_2^f\right)^2 \cdot G_{\tilde{W}^0 \tilde{B}h}^2 \cdot \Omega_h(\mu_{\tilde{B}}, \mu_h), \\
 &\simeq \frac{\alpha^2 M_2}{8\pi} \frac{s_{2\beta}^2}{s_{2W}^2} \frac{m_f^2}{\mu^2} \Omega_h(\mu_{\tilde{B}}, \mu_h), \\
 &\sim \frac{4\alpha^2}{15\pi} \frac{(\Delta M)^5}{m_h^4} \frac{s_{2\beta}^2}{s_{2W}^2} \frac{m_f^2}{\mu^2},
 \end{aligned} \tag{4.4}$$

where $r_2^u = c_\alpha/s_\beta$ and $r_2^d = -s_\alpha/c_\beta$, both of which are reduced to -1 in the decoupling limit of the SUSY Higgses. The $\mu_h = m_h^2/M_2$ and the analytic form of $\Omega_h(x, y)$ is given in Appendix B. In the last step we approximate the expression assuming $\Delta M/M_2 \ll 1$. Up to the contribution induced from the dimension 5 operator, we can approximate $\Gamma^{(2)} \simeq \sum_f \hat{\Gamma}_f^h$. We provide the analytic expression of $\Gamma^{(4)}(\tilde{W}^0 \rightarrow f \bar{f}' \tilde{B})$ in Appendix A

For the large μ region with $|\mu| > 20$ TeV, the total decay rate is dominated by $\Gamma^{(2)}$.

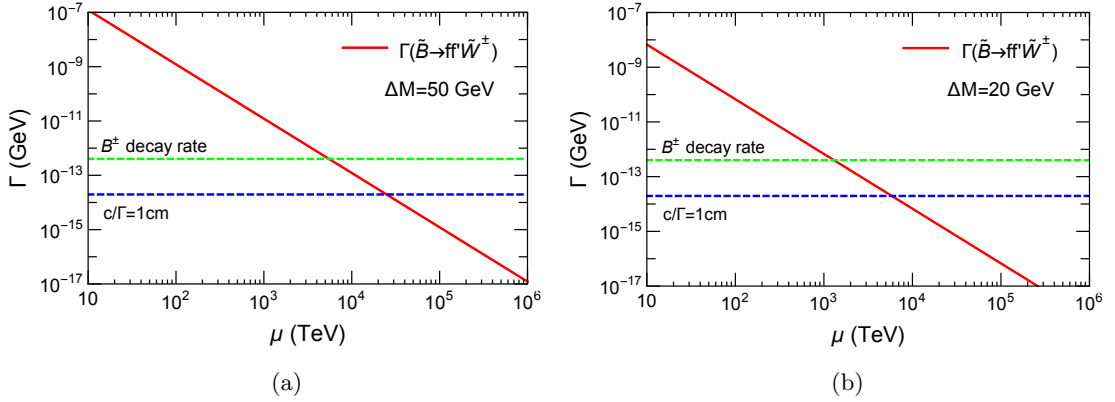


Figure 8. The decay rate of the Bino as a function of $|\mu|$. The other parameters are taken at $M_1 = M_2 + \Delta M$, $M_2 = 500$ GeV, $\tan \beta = 2$.

In this regime, the lifetime of the neutral Wino can be written approximately as

$$c\tau_{\tilde{W}^0} \sim 1 \text{ cm} \cdot \left(\frac{\mu}{10^2 \text{ TeV}} \right)^2 \left(\frac{50 \text{ GeV}}{\Delta M} \right)^5 \left(\frac{1}{s_{2\beta}} \right)^2. \quad (4.5)$$

4.2 Bino NLSP case ($|M_1| > |M_2|$)

In this subsection we assume the Bino is heavier than the Winos and define $\Delta M \equiv |M_1| - |M_2| > 0$. If $\Delta M < m_W$, the Bino decays in three body. As discussed in the previous subsection, the Higgs exchange diagram is suppressed by the mass of final state fermions, and the W exchange diagram for the $\tilde{B} \rightarrow f\bar{f}'\tilde{W}^\pm$ dominates the Bino decay. The partial decay rate can be written as

$$\begin{aligned} \Gamma_f(\tilde{B} \rightarrow f\bar{f}'\tilde{W}^\pm) &= \frac{\alpha^2 M_1}{16\pi} \frac{1}{s_W^2} \cdot G_{\tilde{B}\tilde{W}^\pm W}^2 \cdot \Omega_-(\mu_{\tilde{W}}, \mu_w), \\ &\simeq \frac{\alpha^2 M_1}{16\pi} \frac{s_{2\beta}^2}{s_W^2} \frac{m_Z^2}{\mu^2} \left[\frac{m_W^2 \Omega_-(\mu_{\tilde{W}}, \mu_w)}{(M_1 - M_2)^2} \right], \\ &\sim \frac{4\alpha^2}{15\pi} \frac{(\Delta M)^3}{\mu^2} \frac{s_{2\beta}^2}{s_W^2}, \end{aligned} \quad (4.6)$$

where $\mu_w \equiv m_W/M_1$ and we approximate the expression assuming $\Delta M/M_1 \ll 1$ in the last step.

In Fig. 8(a) and 8(b) we show the Bino decay rate $\Gamma(\tilde{B} \rightarrow ff'\tilde{W}^\pm) = \sum_f \Gamma_f(\tilde{B} \rightarrow ff'\tilde{W}^\pm)$ as a function of $|\mu|$ for $\Delta M = 50$ and 20 GeV, respectively. As can be seen, the Bino becomes long lived for $|\mu| > 10^{3-4}$ TeV depending on ΔM . The approximate formula for the Bino lifetime is given by

$$c\tau_{\tilde{B}} \sim 0.5 \text{ cm} \cdot \left(\frac{\mu}{10^4 \text{ TeV}} \right)^2 \left(\frac{30 \text{ GeV}}{\Delta M} \right)^3 \left(\frac{1}{s_{2\beta}} \right)^2. \quad (4.7)$$

5 Large mass splitting between gauginos and higgsinos

In the previous two sections, we found that the Wino and Bino can be long-lived with $|\mu| \gtrsim \mathcal{O}(10^{5-6})$ TeV for two body decays, and $|\mu| \gtrsim \mathcal{O}(10^{1-4})$ TeV for three body decays. On the other hand, the Wino and Bino masses should be less than $\mathcal{O}(1)$ TeV to be produced at colliders. The long-lived Wino and Bino in this scenario can be observed only if an enormous mass splitting between gauginos and higgsinos is realised.

The higgsino mass, μ , is the only dimension-full parameter in the MSSM Lagrangian. Since it is a supersymmetric mass term, its origin can be different from that for the soft masses of gauginos and scalars. If one does not ask the origin of the μ term and accept the fine tuning in the electroweak symmetry breaking, phenomenologically there is no problem in taking μ at any value.

If μ is very large, the low energy effective Lagrangian is obtained by integrating out the heavy higgsino fields. In doing so, the electroweak gauginos receive the threshold correction from the heavy higgsinos as [13, 14]

$$\Delta M_1^h = \frac{\alpha_1}{4\pi} \frac{3}{5} L, \quad \Delta M_2^h = \frac{\alpha_2}{4\pi} L, \quad (5.1)$$

with

$$L \equiv \frac{\mu m_A^2 s_{2\beta}}{|\mu|^2 - m_A^2} \ln\left(\frac{|\mu|^2}{m_A^2}\right), \quad (5.2)$$

where m_A is the CP-odd Higgs mass. If m_A and μ are the same order and $|\mu| \gtrsim \mathcal{O}(10^3)$ TeV, these threshold corrections exceed $\mathcal{O}(10)$ TeV and the Wino and Bino become out of the collider reach. In order for these corrections to be small and realise the large mass splitting between heavy higgsinos and light gauginos, one needs $m_A \ll |\mu|$. Since m_A is related to μ by

$$m_A^2 = 2|\mu|^2 + m_{H_u}^2 + m_{H_d}^2, \quad (5.3)$$

some unnatural cancelation may be required to accommodate observable long-lived Winos and Binos for $|\mu| \gtrsim \mathcal{O}(10^3)$ TeV.

Alternatively, one would like to attribute the origin of μ to the SUSY breaking. In gravity mediation, μ can be generated as [15, 16]

$$\mu = c m_{3/2}, \quad (5.4)$$

where c is a dimensionless coefficient. In this scenario the gaugino masses receive the anomaly mediated contribution [13, 14],

$$\Delta M_1^{\text{AM}} = \frac{\alpha_1}{4\pi} \frac{33}{5} m_{3/2}, \quad \Delta M_2^{\text{AM}} = \frac{\alpha_1}{4\pi} m_{3/2}, \quad \Delta M_3^{\text{AM}} = -\frac{\alpha_1}{4\pi} 3 m_{3/2}, \quad (5.5)$$

as well as the higgsino threshold correction in eq. (5.1). The size of these correction exceeds $\mathcal{O}(10)$ TeV for $|\mu| \gtrsim \mathcal{O}(10^3)$ TeV. In this scenario, some unnatural cancellation among these contributions may be required for the long-lived Bino and Winos within the collider reach for $|\mu| \gtrsim \mathcal{O}(10^3)$ TeV.

From these considerations one may find the case of the Wino NLSP with $|M_2| - |M_1| < m_Z$ particularly interesting because the neutral Wino can become long-lived for $|\mu| \gtrsim \mathcal{O}(10^{1-2})$ TeV. With $|\mu| \sim \mathcal{O}(10^{1-2})$ TeV, the contributions from the higgsino threshold corrections and the anomaly mediation are of the order of $\mathcal{O}(10^{2-3})$ GeV and a large variety of the Wino and Bino spectrum including compressed spectrum for the three body decays can be naturally achieved by the interplay between these contributions [3, 17–19]. To precisely predict the lifetime of the neutral Wino in this regime, calculation of the Z -exchange diagram induced from the dimensional 5 operator may be necessary. We leave this task for future work.

6 Collider signatures

In supersymmetry with heavy scalars and higgsinos, the Bino cross section is largely suppressed both at hadron and e^+e^- colliders. The Binos may nevertheless be produced from decays of gluinos at hadron colliders. As shown in sections 3 and 4, the lifetime of Bino can become larger than $\mathcal{O}(1)$ cm for $|\mu| \gtrsim \mathcal{O}(10^6)$ TeV if the two body decay is allowed and $|\mu| \gtrsim \mathcal{O}(10^4)$ TeV otherwise.

If squarks are heavy the gluinos may also become long-lived. The gluino lifetime is given by

$$c\tau_{\tilde{g}} = \mathcal{O}(1 \text{ cm}) \cdot \left(\frac{1 \text{ TeV}}{m_{\tilde{g}}}\right)^5 \cdot \left(\frac{10^3 \text{ TeV}}{m_{\tilde{q}}}\right)^4. \quad (6.1)$$

Therefore, if the squark mass has the same scale as that of $|\mu|$, the long-lived Binos is produced from long-lived gluinos. To have the gluino decay well inside the detector, $|\mu|$ and the squark mass cannot be too large.

The Bino can become long-lived with not too large $|\mu|$ ($\sim \mathcal{O}(10^4)$ TeV). In this case the Bino predominantly decays into an off-shell W and a charged Wino. The charged Wino subsequently decays into an off-shell W and the neutral Wino, but this decay may also be long-lived [20, 21]. The charged Wino lifetime in this region is given by

$$c\tau_{\tilde{W}^\pm} \sim 5 \text{ cm} \cdot \left(\frac{\Delta m_{\tilde{W}}}{160 \text{ MeV}}\right)^{-3} \left(1 - \frac{m_\pi^2}{\Delta m_{\tilde{W}}^2}\right)^{-1/2}, \quad (6.2)$$

where the mass splitting $\Delta m_{\tilde{W}} \equiv m_{\tilde{W}^\pm} - m_{\tilde{W}^0}$ can be written as

$$\Delta m_{\tilde{W}}^{\text{tree}} \sim \frac{1}{4} \text{sign}(M_1 M_2) \frac{m_Z^4 s_{2W}^2 s_{2\beta}^2}{\mu^2 |M_2 - M_1|}, \quad (6.3)$$

at tree-level and receives the radiative correction, $\Delta m_{\tilde{W}}^{\text{rad}} \sim 160$ MeV [22]. The long-lived charged Winos are usually searched by looking for the disappearing track signature [23, 24]. If the long-lived Binos carry the charged Winos in the middle of the tracking system (50 mm - 100 mm), the signal can be seen as an appearing-and-disappearing track signature in the detector.

The long-lived Wino can be produced either directly at hadron and e^+e^- colliders or indirectly from prompt/non-prompt decays of gluinos at hadron colliders. The charged

Wino predominantly decays into an on or off-shell W and the LSP Bino. If the decay products of $W^{\pm(*)}$ are reconstructed, the signal may be detected as a kinked tracks in the leptonic $W^{(*)}$ channel or a displaced dijet with a charged track pointing to the secondary vertex in the hadronic $W^{(*)}$ channel.

The neutral Wino predominantly decay into a $h^{(*)}$ and a Bino in most cases. The signal should be detected as the displaced jets/dijet signature. In the region where the neutral Wino is long-lived with $|\mu| \sim \mathcal{O}(10^{1-2})$ TeV, the two body decay is kinematically forbidden and the \tilde{W}^0 decays into a Bino and the off-shell Z , h or left-handed sfermions with a small Bino-Wino mass splitting. Because the decay products of these off-shell particles are soft, the e^+e^- may be ideal to detect the long-lived neutral Wino in this parameter region. At hadron colliders, the search for the displaced $Z^{(*)} \rightarrow \ell\ell$ may also be promising.

7 Conclusion

We investigated a possibility of having long-lived Binos and Winos in SUSY models with heavy scalars and higgsinos. In the parameter region of interest the $SU(2)_L$ and $U(1)_Y$ gaugino sectors are secluded each other with very small mixings proportional to v/μ . In this region, the heavier of Bino and Wino does not interact strongly with the lighter one and its lifetime becomes a collider scale, $c\tau \sim \mathcal{O}(1)$ cm.

We revisited the decays of the Bino and the Wino and found simple formulae for the decay rate and the lifetime, which are valid when the scalars and the higgsinos are much heavier than the gauginos. We have found that the long-lived Bino and Wino emerge when $|\mu| \gtrsim \mathcal{O}(10^{5-6})$ TeV if the two-body decay mode is open and $|\mu| \gtrsim \mathcal{O}(10^{3-4})$ TeV otherwise. One exception is the case with $0 < |M_2| - |M_1| < m_Z$, where the lifetime of the neutral Wino becomes $\mathcal{O}(1)$ cm for $|\mu| \sim \mathcal{O}(10^{1-2})$ TeV, depending on the Wino-Bino mass splitting, because the Higgs exchange diagram is suppressed by the mass of final state fermions.

We briefly discussed how the large mass splitting between gauginos and higgsinos can be achieved. If the origin of μ is independent of the SUSY breaking, the large mass splitting can be realised relatively easily, although the threshold correction from the heavy higgsinos to the gaugino masses needs to be suppressed. On the other hand, if the μ is linked to the SUSY breaking and in particular $|\mu| \sim m_{3/2}$, the contribution from the higgsino threshold correction and the anomaly mediation become significant. However the large splitting is still possible if one accepts the cancellation between these contributions.

We also discussed a possible collider signature for the long-lived Bino and Wino in this scenario. The production of Bino is only possible from the decay of gluinos, although gluinos tend to be also long-lived for $m_{\tilde{q}} \gtrsim \mathcal{O}(10^3)$ TeV. For the long-lived Bino NLSP case, the charged Wino may also be long-lived, because of the very small mass splitting within the Wino multiplet. In the $\tilde{B} \rightarrow W^{\pm(*)}\tilde{W}^\mp$ decay, the Binos may carry the long-lived charged Winos in the middle of the tracking system and the signal can be seen as an appearing-and-disappearing track signature.

For the Wino NLSP case, the production of Winos is possible either directly or indirectly from the gluino decay. The long-lived charged Wino decaying $W^{\pm(*)}$ and \tilde{B} can be

detected. For the long-lived ($\tilde{W}^\pm \rightarrow W^\pm(\tilde{B})$) decay, the kinked track signature from the leptonic $W^{(*)}$ may be promising channel. The hadronic $W^{(*)}$ mode may also be seen as the events with the displaced dijet with a track pointing to the secondary vertex. Detecting the long-lived neutral Wino with $|\mu| \sim \mathcal{O}(10^{1-2})$ TeV may be challenging because the decay products may be soft due to the small Wino-Bino mass splitting. In this case, e^+e^- collider may be ideal to detect the long-lived neutral Wino, otherwise the displaced off-shell $Z^* \rightarrow \ell\ell$ decay may be promising even at hadron colliders.

Acknowledgments

K.S. thanks Satoshi Shirai for useful discussion around the dimension 5 operator. K.S. is supported in part by the London Centre for Terauniverse Studies (LCTS), using funding from the European Research Council via the Advanced Investigator Grant 267352.

A The three body decay rate of the neutral Wino

Up to the higher order Z -exchange contribution induced from the dimension 5 operator in eq. (2.13), the three-body neutral Wino decay into a fermion pair and a Bino can be written as

$$\Gamma(\tilde{W}^0 \rightarrow f\bar{f}'\tilde{B}) \simeq \Gamma^{(2)}(\tilde{W}^0 \rightarrow f\bar{f}'\tilde{B}) + \Gamma^{(4)}(\tilde{W}^0 \rightarrow f\bar{f}'\tilde{B}), \quad (\text{A.1})$$

with

$$\Gamma^{(2)}(\tilde{W}^0 \rightarrow f\bar{f}\tilde{B}) \simeq \sum_f \hat{\Gamma}_f^h, \quad (\text{A.2})$$

$$\Gamma^{(4)}(\tilde{W}^0 \rightarrow f\bar{f}\tilde{B}) \simeq \sum_f \left(\hat{\Gamma}_f^Z + \hat{\Gamma}_f^{\tilde{f}} + \hat{\Gamma}_f^{V\tilde{f}} \right), \quad (\text{A.3})$$

where the analytical form of the Higgs exchange contribution, $\hat{\Gamma}_f^h$, is given in eq. (4.4). The formulae for the Z -exchange contribution, $\hat{\Gamma}_f^Z$, the left-handed sfermion exchange contribution, $\hat{\Gamma}_f^{\tilde{f}}$, and their interference term, $\hat{\Gamma}_f^{V\tilde{f}}$, are given by

$$\hat{\Gamma}_f^Z \simeq \frac{\alpha^2 M_2}{32\pi} \frac{\kappa_Z^f c_{2\beta}^2}{2s_{2W}^2} \frac{m_Z^4}{\mu^4} \Omega_+(\mu_{\tilde{B}}, \mu_Z), \quad (\text{A.4})$$

$$\hat{\Gamma}_f^{\tilde{f}}(\tilde{W}^0 \rightarrow f\bar{f}\tilde{B}) \simeq \frac{\alpha^2 M_2}{32\pi} \hat{\kappa}_f^2 \frac{M_2^4}{m_{\tilde{f}_L}^4} \Omega_f(\mu_{\tilde{B}}), \quad (\text{A.5})$$

$$\hat{\Gamma}_f^{V\tilde{f}}(\tilde{W}^0 \rightarrow f\bar{f}\tilde{B}) \simeq \frac{\alpha^2 M_2}{32\pi} \frac{\hat{\kappa}_f \hat{v}_f c_{2\beta}}{s_{2W}} \frac{M_2^2}{m_{\tilde{f}_L}^2} \frac{m_Z^2}{\mu^2} \Omega_{Vf}(\mu_{\tilde{B}}, \mu_Z), \quad (\text{A.6})$$

in the limit of heavy sfermions and higgsinos, where $\mu_{\tilde{B}} = M_1/M_2$, $\mu_Z = m_Z/M_2$. The $\hat{\kappa}_f$ and \hat{v}_f are given as $\hat{\kappa}_f \simeq |e_{L1}^f||e_{L2}^f|$ and $\hat{v}_f \simeq 4(I_3^f - e_f s_W^2)$, respectively, where I_3^f and e_f are the isospin and the electric charge of the sfermion \tilde{f} . The e_{Li}^f represents the coupling between the left-handed sfermion and the neutralino $\tilde{\chi}_i^0$, which can be written as

$$\begin{pmatrix} e_{L1}^f \\ e_{L2}^f \end{pmatrix} \simeq \sqrt{2} \left[e_f \begin{pmatrix} Z_{11}^* c_W \\ s_W \end{pmatrix} + \frac{I_3^f - e_f s_W^2}{c_W s_W} \begin{pmatrix} -Z_{11}^* s_W \\ c_W \end{pmatrix} \right]. \quad (\text{A.7})$$

The κ_Z^f is given by $\kappa_Z^f \simeq (2I_3^f - 4e_f s_W^2)^2 + (2I_3^f)^2$, namely for each fermion we have

$$\begin{aligned} u &: (1 - \frac{8}{3}s_W^2)^2 + 1 \\ d &: (-1 + \frac{4}{3}s_W^2)^2 + 1 \\ \nu &: 2 \\ e &: (-1 + 4s_W^2)^2 + 1. \end{aligned} \quad (\text{A.8})$$

B The functions

We summarize the functions we used.

$$f_{\pm}(x, y) = \sqrt{\lambda(x, y)}\eta_{\pm}(x, y), \quad (\text{B.1})$$

$$\lambda(x, y) = 1 + x^2 + y^2 - 2x - 2y - 2xy, \quad (\text{B.2})$$

$$\eta_{\pm}(x, y) = (1 + x - y) + \frac{(1 - x + y)(1 - x - y)}{y} \pm 6\sqrt{x}, \quad (\text{B.3})$$

$$f_h(x, y) = (1 + x - y + 2\sqrt{x})\sqrt{\lambda(x, y)}, \quad (\text{B.4})$$

$$\Omega_{\pm}(x, y) = 2F(x, y) \pm G(x, y), \quad (\text{B.5})$$

$$\begin{aligned} F(x, y) &= \frac{x - 1}{6y}[\omega(x, y) + y(5 + 5x - 7y)] \\ &\quad - \frac{y}{2}\{(1 + x - y)\ln x + [\omega(x, y) + 2x]\mathcal{L}(x, y)\}, \end{aligned} \quad (\text{B.6})$$

$$G(x, y) = \sqrt{x}[4(x - 1) + (1 + x - 2y)\ln x + \{\omega(x, y) - y(1 + x - y)\}\mathcal{L}(x, y)], \quad (\text{B.7})$$

$$\omega(x, y) = 1 - 2x - 2y + (y - x)^2, \quad (\text{B.8})$$

$$\mathcal{L}(x, y) = \frac{2}{\sqrt{-\omega(x, y)}} \left[\arctan\left(\frac{-1 + x - y}{\sqrt{-\omega(x, y)}}\right) - \arctan\left(\frac{1 - x - y}{\sqrt{-\omega(x, y)}}\right) \right], \quad (\text{B.9})$$

$$\Omega_h(x, y) = H(x, y) + G(x, y), \quad (\text{B.10})$$

$$\begin{aligned} H(x, y) &= \frac{1}{2}(1 - x)(6y - 5 - 5x) + \frac{1}{2}(1 - 4y - 4xy + 3y^2 + x^2)\ln x \\ &\quad + \frac{1}{2}(-5x^2y - 3y^3 + 7y^2 + 1 - x^2 - x + x^3 - 5y + 7xy^2 - 2xy)\mathcal{L}(x, y), \end{aligned} \quad (\text{B.11})$$

$$\begin{aligned} \Omega_f(x) &= \frac{1}{6}(1 - 8x + 8x^3 - x^4 - 12x^2\ln x) \\ &\quad + \frac{\sqrt{x}}{6}[1 + x(9 - 9x - x^2) + 6x(1 + x)\ln x], \end{aligned} \quad (\text{B.12})$$

$$\begin{aligned}\Omega_V(x) = & \frac{1}{36} \left(-5 - 9x + 9x^2 + 5x^3 + (3 - 9x - 18x^2) \ln x \right) \\ & - \frac{(x-1)\sqrt{4x-1}}{6} \left[\arctan\left(\frac{1}{\sqrt{4x-1}}\right) + \arctan\left(\frac{1-2x}{\sqrt{4x-1}}\right) \right].\end{aligned}\quad (\text{B.13})$$

$$\begin{aligned}\Omega_{Vf}(x, y) = & (1 + \sqrt{x}) \left[\right. \\ & \left. [1 - 3x - 3x^2 + x^3 - 3(1+x)y^2 + 2y^3] \frac{\ln x}{12} + [5 + 5x^2 - 12(y-1)y + 2x(1+6y)] \frac{x-1}{36} \right. \\ & \left. + [1 + x^2 + x(y-2) + y - 2y^2] [x^2 + (y-1)^2 - 2x(1+y)] \frac{\mathcal{M}(x, y)}{6\sqrt{-x^2 - (y-1)^2 + 2x(1+y)}} \right],\end{aligned}\quad (\text{B.14})$$

$$\mathcal{M}(x, y) = \arctan\left[\frac{-1 + x + y}{\sqrt{-x^2 - (y-1)^2 + 2x(1+y)}}\right] - \arctan\left[\frac{1 - x + y}{\sqrt{-x^2 - (y-1)^2 + 2x(1+y)}}\right].\quad (\text{B.15})$$

References

- [1] G. F. Giudice and A. Strumia, Nucl. Phys. B **858** (2012) 63 [arXiv:1108.6077 [hep-ph]].
- [2] M. Ibe, S. Matsumoto and T. T. Yanagida, Phys. Rev. D **85** (2012) 095011 [arXiv:1202.2253 [hep-ph]].
- [3] E. Bagnaschi, G. F. Giudice, P. Slavich and A. Strumia, JHEP **1409** (2014) 092 [arXiv:1407.4081 [hep-ph]].
- [4] N. Arkani-Hamed and S. Dimopoulos, JHEP **0506** (2005) 073 [hep-th/0405159].
- [5] J. Hisano, S. Matsumoto, M. Nagai, O. Saito and M. Senami, Phys. Lett. B **646** (2007) 34 [hep-ph/0610249].
- [6] M. Cirelli, A. Strumia and M. Tamburini, Nucl. Phys. B **787** (2007) 152 [arXiv:0706.4071 [hep-ph]].
- [7] J. L. Hewett, B. Lillie, M. Masip and T. G. Rizzo, JHEP **0409** (2004) 070 [hep-ph/0408248].
- [8] G. Aad *et al.* [ATLAS Collaboration], Phys. Rev. D **88** (2013) 11, 112003 [arXiv:1310.6584 [hep-ex]].
- [9] J. F. Gunion and H. E. Haber, hep-ph/9301205.
- [10] A. Djouadi, Y. Mambrini and M. Muhlleitner, Eur. Phys. J. C **20** (2001) 563 [hep-ph/0104115].
- [11] V. Khachatryan *et al.* [CMS Collaboration], Phys. Rev. D **91** (2015) 1, 012007 [arXiv:1411.6530 [hep-ex]].
- [12] G. Aad *et al.* [ATLAS Collaboration], Phys. Lett. B **743** (2015) 15 [arXiv:1501.04020 [hep-ex]].
- [13] L. Randall and R. Sundrum, Nucl. Phys. B **557** (1999) 79 [hep-th/9810155].

- [14] G. F. Giudice, M. A. Luty, H. Murayama and R. Rattazzi, JHEP **9812** (1998) 027 [hep-ph/9810442].
- [15] G. F. Giudice and A. Masiero, Phys. Lett. B **206** (1988) 480.
- [16] K. Inoue, M. Kawasaki, M. Yamaguchi and T. Yanagida, Phys. Rev. D **45** (1992) 328.
- [17] B. Bhattacherjee, B. Feldstein, M. Ibe, S. Matsumoto and T. T. Yanagida, Phys. Rev. D **87** (2013) 1, 015028 [arXiv:1207.5453 [hep-ph]].
- [18] L. J. Hall, Y. Nomura and S. Shirai, JHEP **1301** (2013) 036 [arXiv:1210.2395 [hep-ph]].
- [19] K. Harigaya, K. Kaneta and S. Matsumoto, Phys. Rev. D **89** (2014) 11, 115021 [arXiv:1403.0715 [hep-ph]].
- [20] M. Ibe, T. Moroi and T. T. Yanagida, Phys. Lett. B **644** (2007) 355 [hep-ph/0610277].
- [21] M. R. Buckley, L. Randall and B. Shuve, JHEP **1105** (2011) 097 [arXiv:0909.4549 [hep-ph]].
- [22] M. Ibe, S. Matsumoto and R. Sato, Phys. Lett. B **721** (2013) 252 [arXiv:1212.5989 [hep-ph]].
- [23] G. Aad *et al.* [ATLAS Collaboration], Phys. Rev. D **88** (2013) 11, 112006 [arXiv:1310.3675 [hep-ex]].
- [24] V. Khachatryan *et al.* [CMS Collaboration], JHEP **1501** (2015) 096 [arXiv:1411.6006 [hep-ex]].